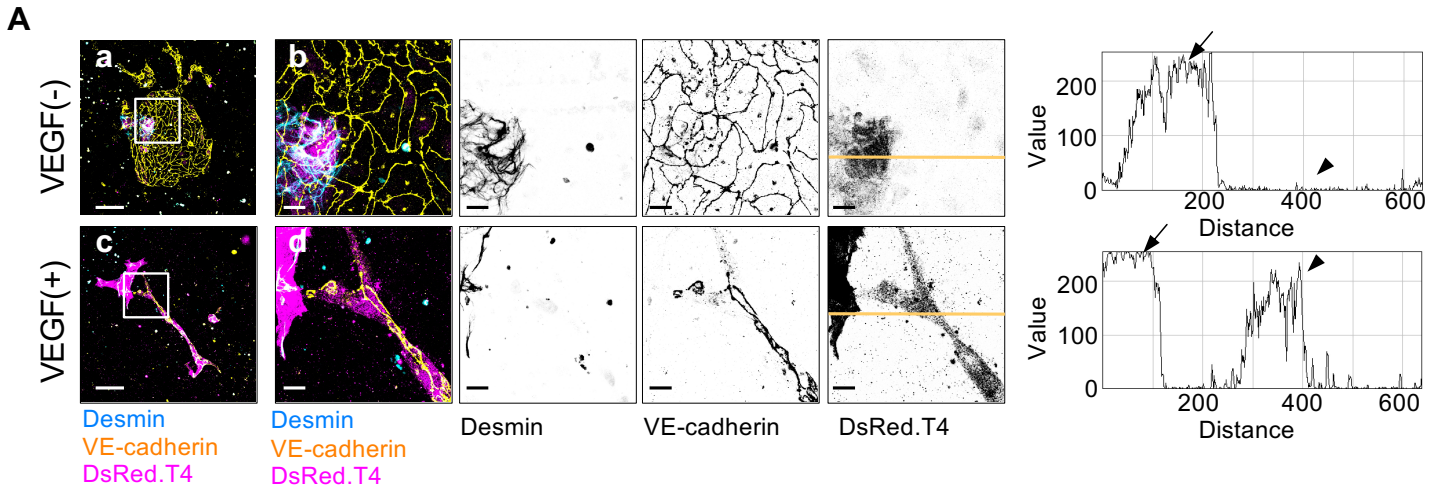

Figure S1. The *Tagln* promoter is activated in ECs stimulated with VEGF

KDR$^+$ cells induced from F10-EGFP/Tagln-DsRed.T4 ESCs were cultured on an OP9 cell layer for four days with or without addition of VEGF (10 ng/ml). We obtained z-stack confocal images of cultures after fixation and immunostaining. (A) Immunostaining of desmin (cyan), VE-cadherin (yellow) and DsRed.T4 (magenta). Multiple or individual channels are shown as merged or black-white inverted images, respectively. Panels (b) and (d) show higher magnifications of the boxed area in panels (a) and (c), respectively. Scale bars indicate 100 µm (a and c) or 20 µm (b and d). The right panels show the fluorescence intensity profiles along each yellow line in the DsRed.T4 image. Arrows and arrowheads indicate the peaks of SMCs and ECs, respectively. Similar results were obtained in three independent experiments using two clones. (B) ECs were categorized into the two types of EC shape: cobblestone (type cob) and elongated (type elong), and scored as either Desmin+ or Desmin−. The proportion of Desmin− and Desmin+ ECs with the two types of EC shape are shown. The total number of ECs of each shape for the two VEGF treatments, observed across three independent experiments using different clones, is indicated in the brackets.

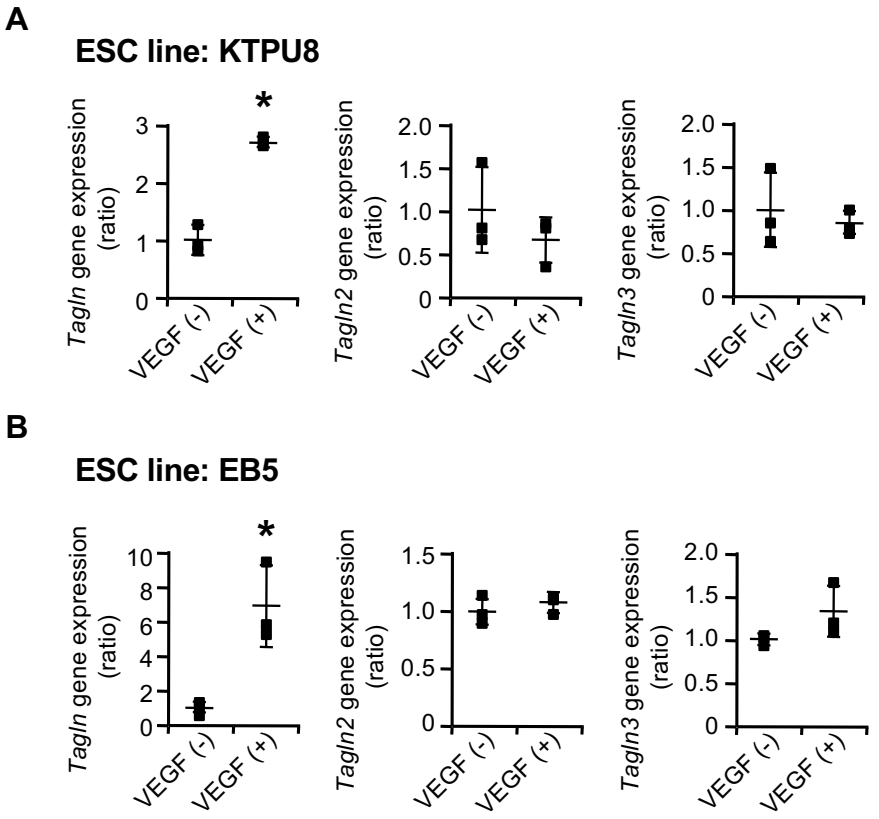

Figure S2. Expressions of *Tagln* isoforms in ECs derived from ESCs

KDR^{+} cells induced from two mouse ESC lines, KTPU8 and EB5, were cultured on an OP9 cell layer with or without the addition of VEGF (10 ng/ml). After four days, CD45^{-} VE-cadherin^{+} CD31^{+} KDR^{+} ECs were purified. (A and B) Expressions of the *Tagln, Tagln2 and Tagln3* genes in ECs derived from KTPU8 (A) and EB5 (B) were quantified using real-time quantitative PCR. Expression levels were normalized to *B2m*. Data is presented as a ratio relative to the VEGF (-) control (mean ± SD, n = 3 from three independent experiments). The Data were analyzed using F-test, followed by a two-tailed t-test (* $p < 0.05$).

A

***TAGLN* (WT)**

GGATCATAGTGCAGTGTGGCCCTGATGTGGGC**CGCCCAGACCGTGGGCGCTTGGG**CTTCCAGGTCTGGC

***SM22* (8-bp deletion)**

GGATCATAGTGCAGTGTGGCCCTGATGTGGGC**CGCCCAGACCGT**-------- **GGG**CTTCCAGGTCTGGC

***TAGLN2* (WT)**

CAGATCCTGATCCAGTGGATCACCACCCAGTG**CCGAAAGGATGTGGGCCGGCCCC**AGCCTGGACGCGAG

***Tagln2* (32-bp deletion)**

CAGATCCTGATCCAG---------- **CCGGCCCC**AGCCTGGACGCGAG

***TAGLN3* (WT)**

GATGCGGACCTGGAGAACAAGCTGGTGGACTG**GATCATCCTGCAGTGCGCCG**AGGACATAGAGCACCCG

***Tagln3* (10-bp deletion)**

GATGCGGACCTGGAGAACAAGCTGGTGGACTG**GATCATCCTGCAGTGCG**---------- AGAGCACCCG

B

***TAGLN* (8-bp deletion)**

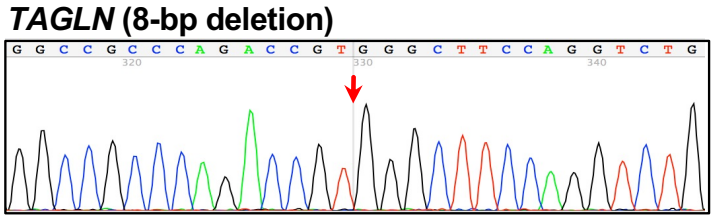

***TAGLN2* (32-bp deletion)**

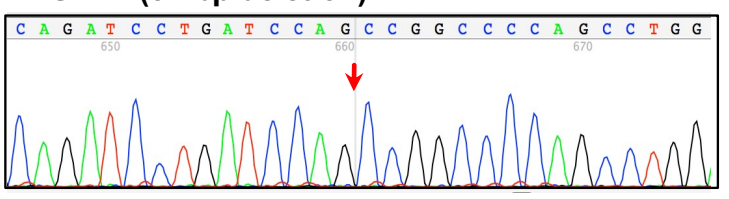

***TAGLN3* (10-bp deletion)**

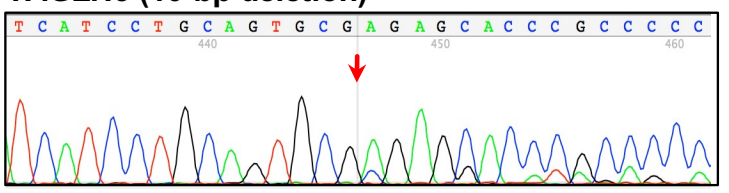

C

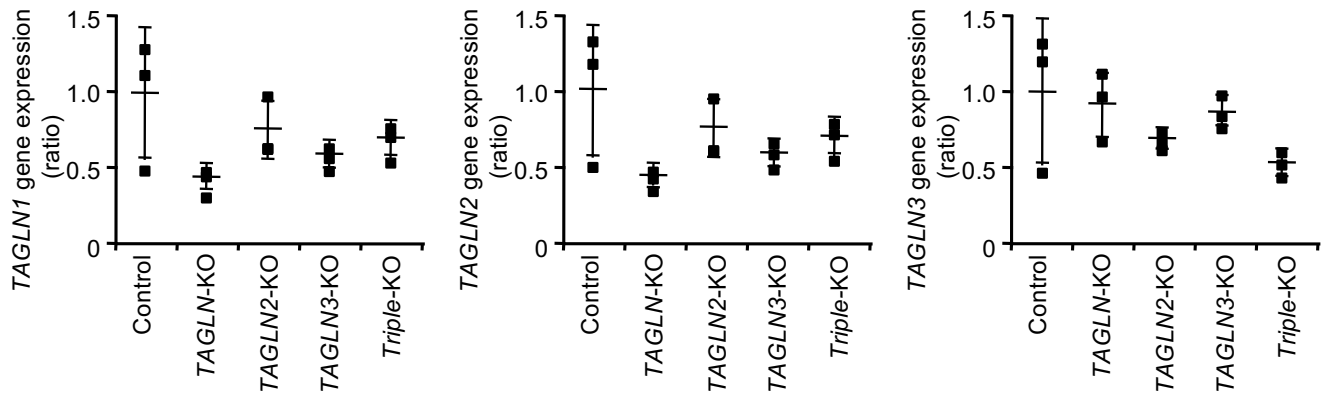

Figure S3. CRISPR/Cas9-mediated mutagenesis of the *TAGLN* isoforms

(A) Sequences of wild type (WT) and the representative mutations at target sites of genome editing in *TAGLN*, *TAGLN2* and *TAGLN3* genes. The target sequence and the PAM region are indicated in blue and red, respectively. Dashes (-) indicate deletions. (B) Nucleotide peaks of the representative mutated sequence at target sites of *TAGLN*, *TAGLN2* and *TAGLN3* genes. Red arrows indicate the location of mutations. (C) HUVECs were genetically edited in *TAGLN*, *TAGLN2* and *TAGLN3* genes with CRISPR/Cas9 system, which indicated as follows: *TAGLN*, *TAGLN2*, *TAGLN3* single-KO (KO), *TAGLN* isoforms triple-KO (triple-KO). The mRNA expression level of *TAGLN* isoforms was determined using real-time quantitative PCR analysis. Data were normalized to *B2M*, and are presented as fold change relative to the control (mean ± SD, n = 3 from three independent experiments). Data were analyzed using Tukey's test. No significant difference was found. These primers used for *TAGLN* isoforms target the downstream regions of CRISPR targeting sites in each gene. The amplification of fragments was not affected by each gene knockout.

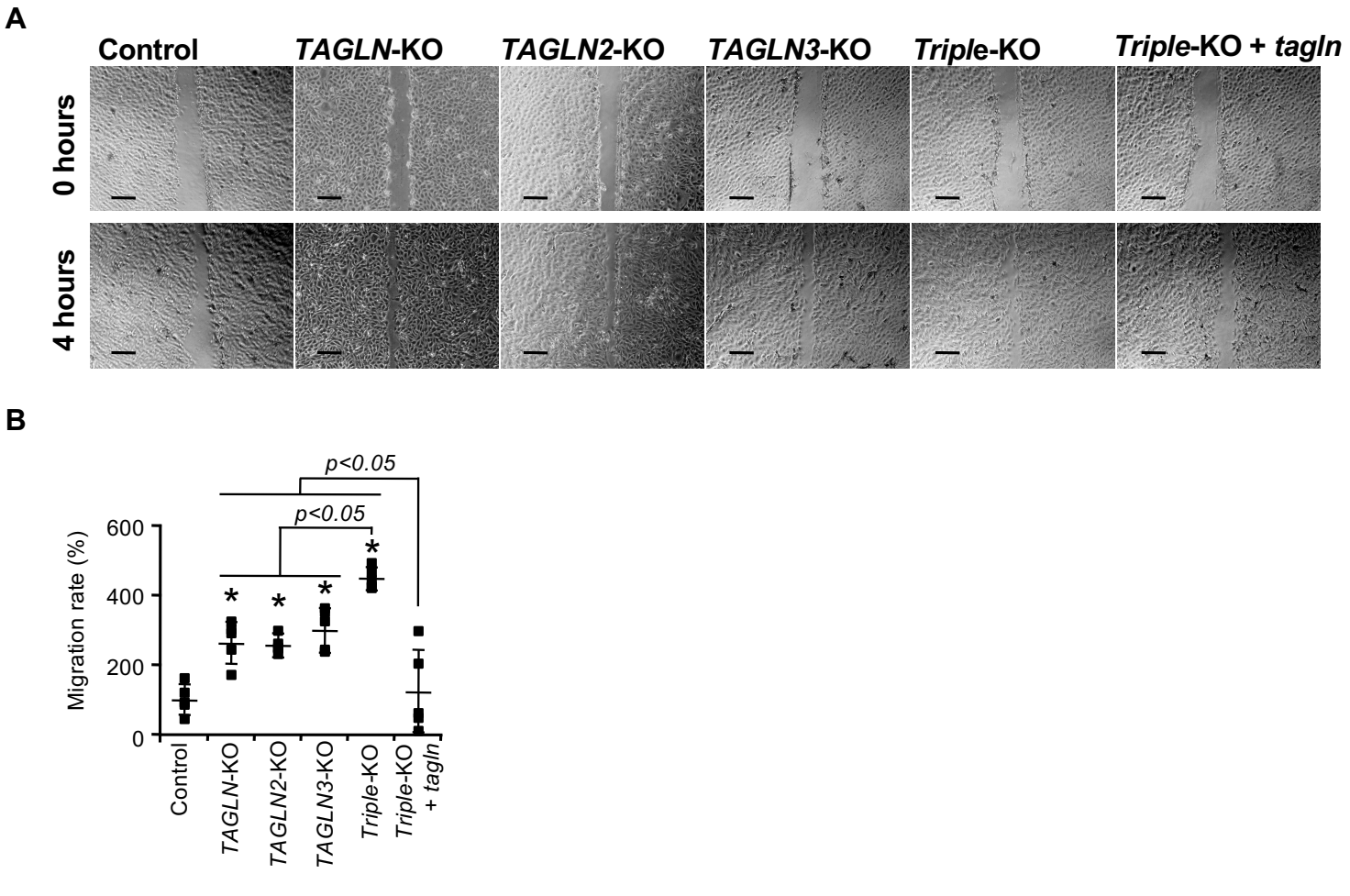

Figure S4. Single and triple-knockout of *TAGLN* isoforms promotes migration of ECs.

HUVECs were genetically edited in *TAGLN*, *TAGLN2* and *TAGLN3* genes with CRISPR/Cas9 system, and applied to rescue expression of zebrafish *tagln*, which indicated as follows: *TAGLN*, *TAGLN2*, *TAGLN3* single-KO (KO), *TAGLN* isoforms triple-KO (triple-KO), and *tagln*-expression-rescued triple-KO (triple-KO + *tagln*). The cell monolayers were scratched using a universal cell scraper. (A) Phase-contrast images at 0 and 4 hours after scratch generation. Scale bars indicate 200 μm. Similar results were obtained in five independent experiments. (B) The migration rate are presented as the mean ± SD (n = 5 from five independent experiments). Data were analyzed using Tukey's test (* $p < 0.05$ compared with the control).

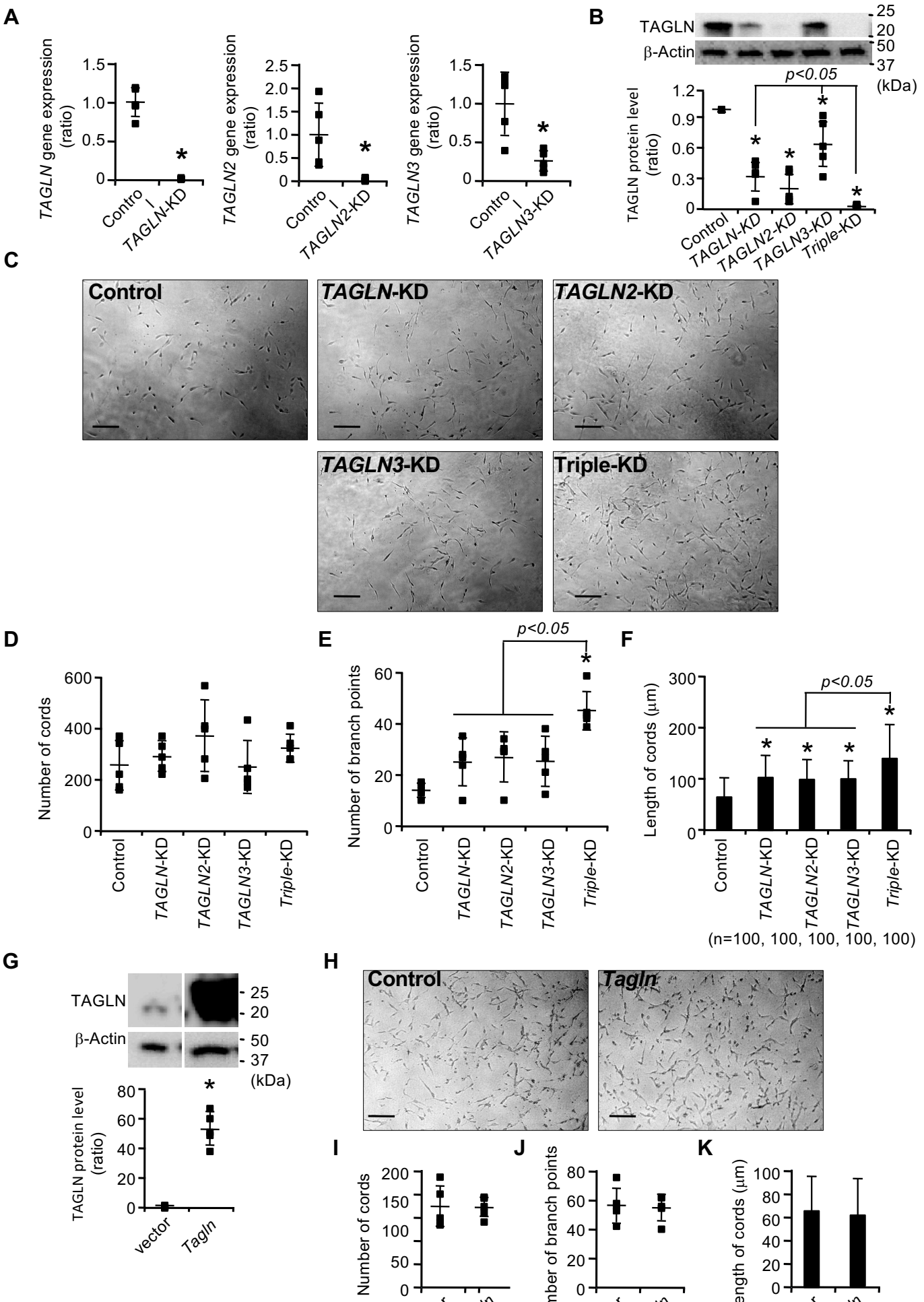

Figure S5. Single and triple-knockdown of *TAGLN* isoforms causes excessive cord-like structure formation
(A-F) HUVECs were transfected with a single siRNA targeting *TAGLN, TAGLN2* or *TAGLN3* (44 pg), a mixture of *TAGLN* isoforms siRNAs (44 pg each, total 132 pg), or control siRNA (132 pg), which indicated as follows: *TAGLN*, *TAGLN2*, *TAGLN3* single-knockdown (KD), and *TAGLN* isoforms triple-KD (triple-KD). (A) The mRNA expression level of *TAGLN* isoforms was determined using real-time quantitative PCR analysis. Data were normalized to *B2M,* and are presented as fold change relative to the control (mean ± SD, n = 5 from five independent experiments). The data were analyzed using F-test, followed by a two-tailed t-test (* $p < 0.05$). (B) Western blot analysis with antibodies against the TAGLN protein (ab14106, Abcam). (Upper) Western blot images. β-Actin protein was used as an internal control. Similar results were obtained in five independent experiments. (Lower) Expression levels were normalized to β-Actin. Data are presented as a ratio relative to the control group (mean ± SD, n = 5 from five independent experiments). The data were analyzed using Tukey's test (* $p < 0.05$ compared with the control group). (C–F) siRNA-transfected HUVECs were grown in 3D sandwich culture in the presence of VEGF (10 ng/ml) for one day. (C) Phase-contrast images. Scale bars indicate 200 μm. Similar results were obtained in three independent experiments. (D and E) The number of cord-like structure (D) and branch points (E) per field is presented as the mean ± SD (n = 5 fields per group). The data were analyzed using Tukey's test (* $p < 0.05$ compared with the control). (F) The length of the cord-like structure is presented as the mean ± SD. The total number of cords examined is indicated in the brackets. The data were analyzed using Tukey's test (* $p < 0.05$ compared with the control). (G-K) HUVECs were transfected with pCAG-Ipuro expressing mouse *Tagln* or pCAG-Ipuro vector. (G) Western blot analysis with antibodies against the TAGLN protein (ab14106, Abcam). (Upper) Western blot images. β-Actin protein was used as an internal control. Similar results were obtained in five independent experiments. (Lower) Expression levels were normalized to β-Actin. Data are presented as a ratio relative to the control group (mean ± SD, n = 5 from five independent experiments). The data were analyzed using F-test, followed by a two-tailed t-test (* $p < 0.05$). (H–K) *Tagln*-transfected HUVECs were grown in 3D sandwich culture in the
presence of VEGF (10 ng/ml) for one day. (H) Phase-contrast images. Scale bars indicate 200 μm. Similar results were obtained in three independent experiments. (I and J) The number of cord-like structure (I) and branch points (J) per field is presented as the mean ± SD (n = 5 fields per group). The data were analyzed using F-test, followed by a two-tailed t-test. (K) The length of the cord-like structure is presented as the mean ± SD. The total number of cords examined is indicated in the brackets. The data were analyzed using F-test, followed by a two-tailed t-test.

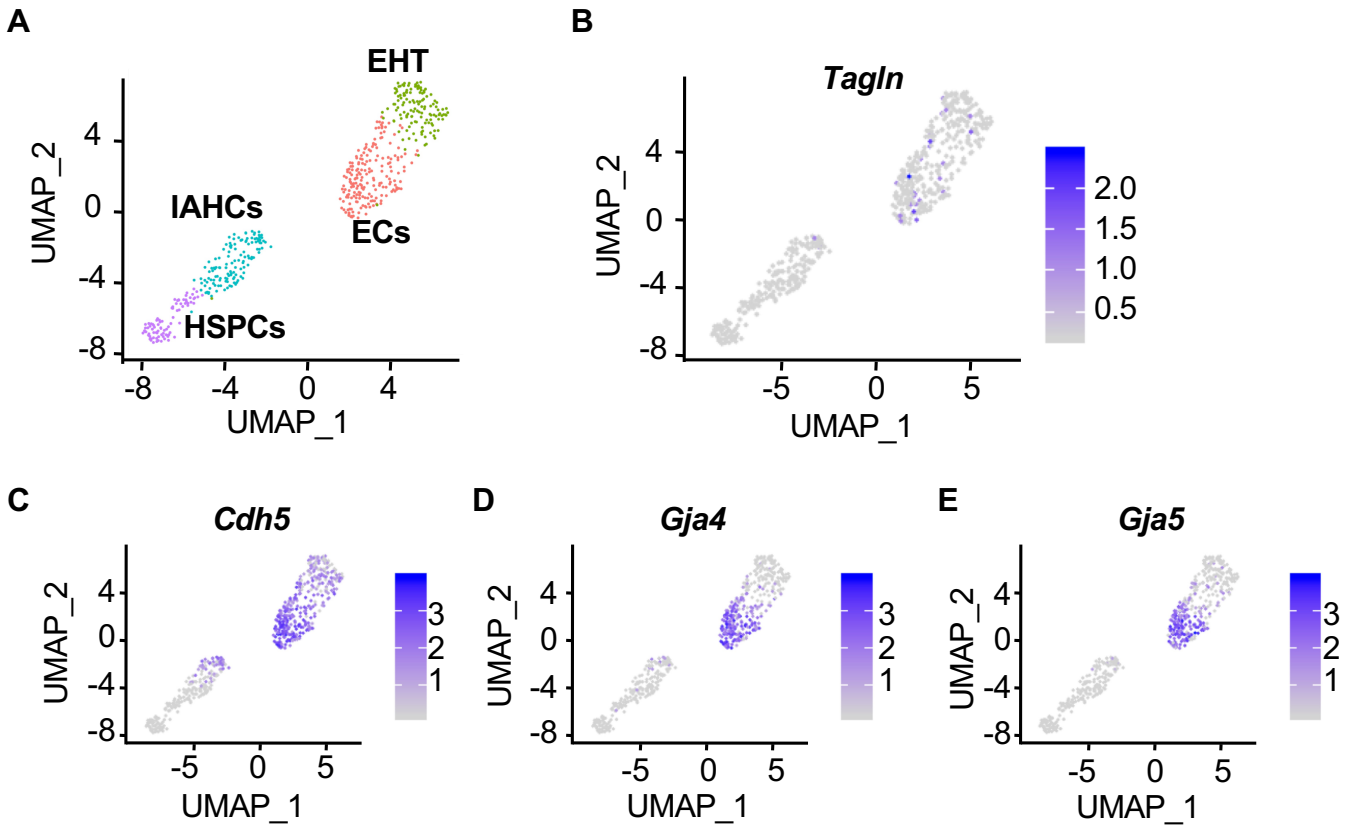

Figure S6. *Tagln*-expressing cells are detected in the EC cluster from embryonic aortas

Analysis of a single cell RNA-seq dataset of E10.5 mouse embryonic aortas. (A) Canonical cell markers were used to label clusters by cell identity based on the previous report (Baron et al., 2018) as represented in the UMAP plot. ECs: endothelial cells, EHT: endothelial-to-hematopoietic transition, IAHCs: intra-aortic hematopoietic clusters, HSPCs: hematopoietic stem and progenitor cells. (B, C, D and E) The feature plot shows the expression of *Tagln* (B) and endothelial cell markers, *Cdh5* (C), *Gja4* (D) and *Gja5* (E).

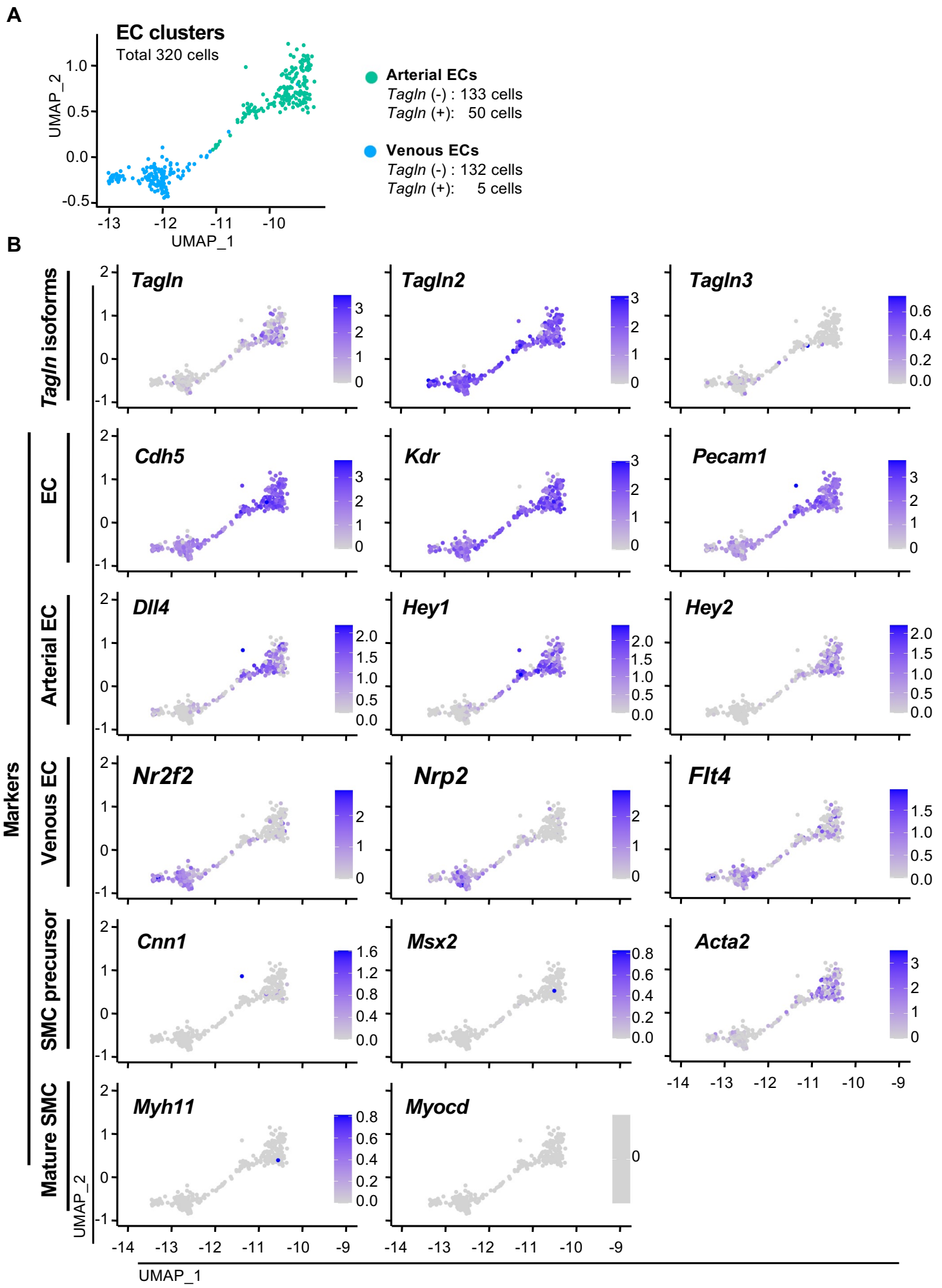
A
EC clusters
Total 320 cells
UMAP_2
UMAP_1
Arterial ECs
Tagln (-) : 133 cells
Tagln (+): 50 cells
Venous ECs
Tagln (-) : 132 cells
Tagln (+): 5 cells
B
Markers
Tagln isoforms
EC
Arterial EC
Venous EC
SMC precursor
Mature SMC
Tagln
Tagln2
Tagln3
Cdh5
Kdr
Pecam1
Dll4
Hey1
Hey2
Nr2f2
Nrp2
Flt4
Cnn1
Msx2
Acta2
Myh11
Myocd
UMAP_2
UMAP_1

Figure S7. *Tagln*-expressing cells are detected in the arterial and venous EC clusters

Analysis of a single cell RNA-seq dataset of the AGM region and the FL of an E10.5 mouse embryo. (A) Arterial and venous EC clusters in the total EC cluster. The green dots show arterial ECs. The blue dots show venous ECs. (B) The feature plots show the expression of *Tagln* isoforms, and markers for EC, arterial EC, venous EC, SMC precursor and mature SMC. Canonical cell markers were based on the previous reports (Chang et al., 2012) (for a review, see (Heinke et al., 2012)).

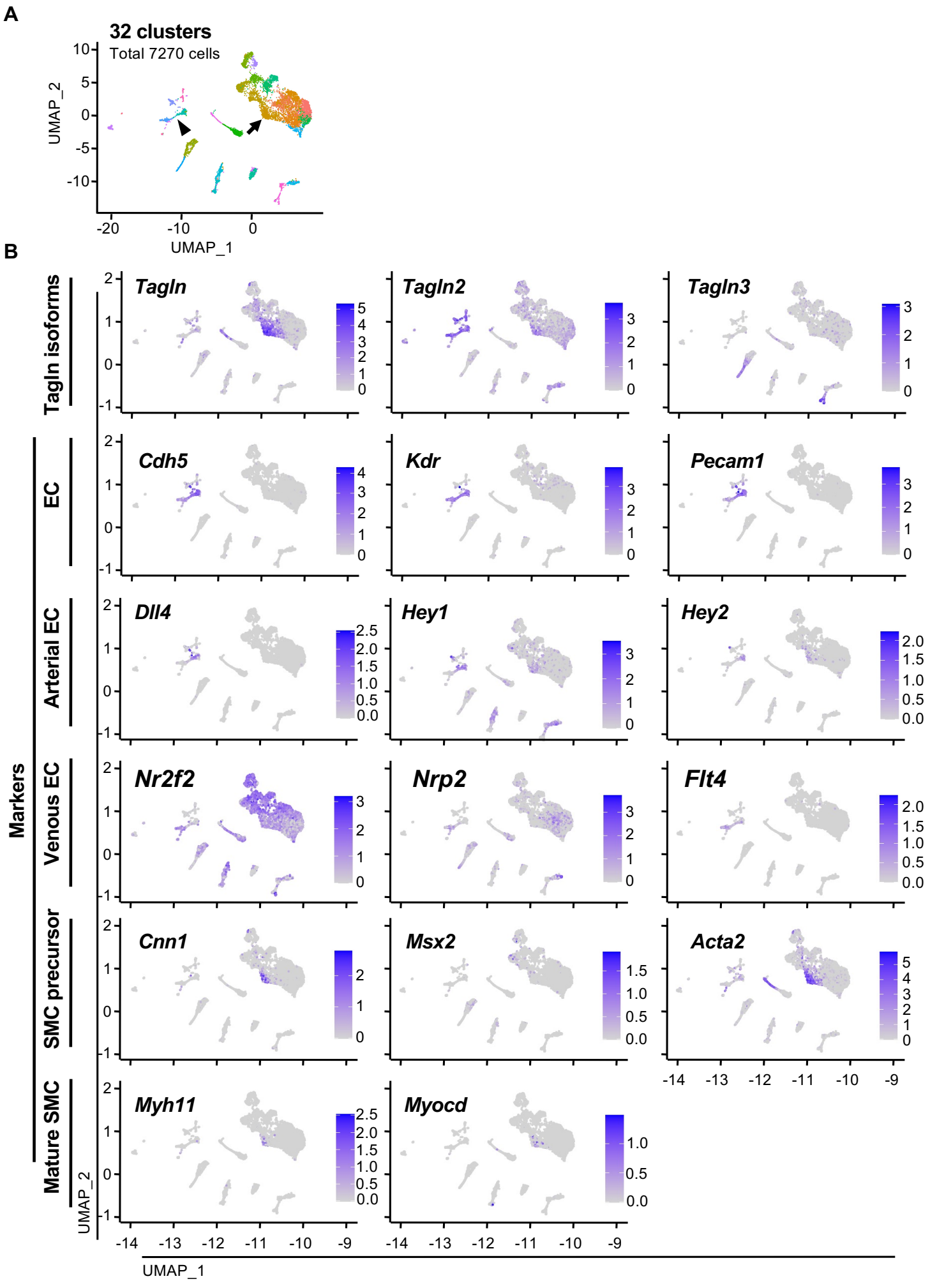

Figure S8. *Tagln* -expressing cells are detected in both EC and SMC clusters. Analysis of a single cell RNA-seq dataset of the AGM region and the FL of an E10.5 mouse embryo. (A) Total 32 clusters. The arrowhead points to the total EC cluster shown in Supplementary figure 7. The arrow points to the SMC cluster. (B) The feature plots show the expression of *Tagln* isoforms, and markers for EC, arterial EC, venous EC, SMC precursor and mature SMC.

Table S1. List of genes highly expressed in *Tagln* -positive ECs in embryonic aortas

gene	avg_logFC
Tagln	1.298254105
Acta2	1.252795771
Eln	1.225094955
Fbln5	0.652144013
Car4	0.635177264
Lamc1	0.542729891
Reg3b	0.53645699
Pdlim3	0.490619397
Slc2a1	0.488762541
Igfbp7	0.472637949
Lsr	0.463220813
Myl12a	0.456294191
Wbp1	0.447633409
Hmg20a	0.440111165
Tpm1	0.440099826
St3gal5	0.435698182
Mcts1	0.43517988
Fbln2	0.431716937
Tm4sf1	0.429455732
Tie1	0.425069231
Col3a1	0.424927296
Kras	0.423854609
Cdkn1c	0.422729154
Chtf8	0.419118954
Jam3	0.416155381
Hipk3	0.409065587
Rtf1	0.400691343
Mrpl4	0.398818005
Ash2l	0.396356419
8430408G22Rik	0.396146909
Ist1	0.390825899
Wdr26	0.387434777

gene	avg_logFC
Slc22a23	0.386482734
Trim27	0.384438805
Impdh1	0.379036697
Rnf215	0.379026475
Phf14	0.377817685
Tgfb1i1	0.375543426
Drap1	0.374364313
Dtx2	0.371840362
Zc3h7a	0.371799869
Btg2	0.371518371
Dnajb4	0.367692871
Gata2	0.365689289
Poc1b	0.363878479
Dnajc3	0.362934149
Mrpl51	0.362207936
Myadm	0.362163692
Flna	0.361683614
S100a11	0.360985408
Frmd8	0.360441406
Rai14	0.359601271
Tmem2	0.359134366
Pan3	0.358562311
9530068E07Rik	0.357045698
Phf20l1	0.356027931
Slc31a1	0.353012216
Yipf6	0.35104851
Il15	0.351024636
Gns	0.350236307
Lsmd1	0.349790844
Qk	0.34419299
Golt1b	0.343473095
Riok2	0.342806516

gene	avg_logFC
Hsd17b10	0.34172693
Pbdc1	0.341083816
Prnd	0.341019554
Khdrbs3	0.339911471
Ensa	0.339244925
Galnt2	0.339067826
Unc5b	0.338496426
Fbxl20	0.338239246
Cacna1a	0.336892608
Pdhb	0.336789987
Csrp2	0.335267949
Chd6	0.334486059
Col4a1	0.332944567
Pnpla2	0.332778986
Urod	0.332622693
Itgb1	0.330644585
Scube1	0.330501609
Capn2	0.3298931
Bptf	0.32870413
Dcaf12l1	0.328407283
Hps5	0.328271059
Igf2r	0.32817896
Acvr1	0.327801119
Kdm2b	0.327784046
Rnasek	0.32716961
Pja2	0.326442668
Ajuba	0.325255251
Tnfaip2	0.325212424
Myo1c	0.323585563
Nfib	0.323081132
Rras	0.322059865

Table S2. List of gene ontology (OG) associated with genes in Supplementary table 1

GO biological process complete	Fold Enrichment	raw P-value	FDR
angiogenesis (GO:0001525)	7.06	0.0000065	0.020500
blood vessel morphogenesis (GO:0048514)	5.74	0.0000114	0.022400
tube morphogenesis (GO:0035239)	4.42	0.0000083	0.018800
head development (GO:0060322)	4.37	0.0000214	0.037500
tube development (GO:0035295)	4.21	0.0000012	0.019300
anatomical structure formation involved in morphogenesis (GO:0048646)	3.97	0.0000056	0.029700
anatomical structure morphogenesis (GO:0009653)	2.66	0.0000069	0.018200
cellular component organization (GO:0016043)	1.94	0.0000051	0.040100
cellular component organization or biogenesis (GO:0071840)	1.92	0.0000062	0.024300

Table S3. List of genes highly expressed in *Tagln*-positive ECs from AGM and FL

The asterisks are the genes shown in supplementary table 1.

	gene	avg_logFC
*	Tagln	2.20949927
*	Acta2	1.7442024
	Actc1	1.06343492
*	Tpm1	0.91730392
	Myl9	0.88662588
*	Btg2	0.61183573
	Lgals1	0.52584705
	Prdx4	0.52543552
	Tmem100	0.515779
	Txnip	0.51104832
	Spon2	0.47752857
	Sptlc2	0.46808485
	Fn1	0.44640552
	Loxl2	0.44529066
	Klf2	0.44072027
*	S100a11	0.44052715
	Fbn1	0.42912497
	Ccnd2	0.42771652
	Cd63	0.42633846

gene	avg_logFC
Fchsd2	0.40561415
Klf4	0.40494123
Mmp2	0.39937238
Adgrg6	0.3928397
Col5a2	0.3788074
Vwf	0.36763662
Slit2	0.36753451
Vps4a	0.3669577
Pmp22	0.35555139
Clu	0.35219103
AU021092	0.34454944
Ptn	0.34017416
Nrp1	0.34008331
Htra1	0.33946908
Col26a1	0.33411637
Smpdl3a	0.33351794
Tmem120a	0.33328635
Gjc1	0.3307873
Alox12	0.32942225

Table S4. List of OG associated with genes in Supplementary table 3 The asterisks are the GO terms shown in Supplementary table 2.

	GO biological process complete	Fold Enrichment	raw P-value	FDR
	AV node cell to bundle of His cell communication by electrical coupling	> 100	0.0000320	0.01230
	cell communication by electrical coupling involved in cardiac conduction	> 100	0.0000480	0.01760
	regulation of retinal ganglion cell axon guidance	> 100	0.0000671	0.02200
	cellular response to laminar fluid shear stress	> 100	0.0000894	0.02710
	neural crest cell migration involved in autonomic nervous system develop	> 100	0.0001150	0.03060
	gap junction assembly	> 100	0.0001150	0.03010
	response to laminar fluid shear stress	> 100	0.0001150	0.02960
	neuron projection extension involved in neuron projection guidance	> 100	0.0001430	0.03530
	axon extension involved in axon guidance	> 100	0.0001430	0.03470
	cell communication by electrical coupling	> 100	0.0001430	0.03420
	actin-myosin filament sliding	> 100	0.0001750	0.03880
	dendrite arborization	> 100	0.0002100	0.04400
	AV node cell to bundle of His cell communication	99.95	0.0002480	0.04810
	positive regulation of nitric oxide biosynthetic process	35.09	0.0001020	0.02880
	positive regulation of nitric oxide metabolic process	34.36	0.0001090	0.03000
*	sprouting angiogenesis	28.43	0.0001860	0.04060
	positive regulation of reactive oxygen species biosynthetic process	26.6	0.0002240	0.04580
	endothelial cell migration	25.37	0.0002560	0.04860
	positive regulation of cell-substrate adhesion	16.53	0.0001100	0.02990
	cardiac chamber morphogenesis	15.59	0.0001370	0.03420
	positive regulation of chemotaxis	15.06	0.0001560	0.03610
	ameboidal-type cell migration	14.47	0.0000264	0.01120
	mesenchymal cell differentiation	13.92	0.0002100	0.04460
	negative regulation of neuron projection development	13.49	0.0002350	0.04630
	regulation of endothelial cell migration	13.01	0.0002690	0.04990
	heart morphogenesis	12.45	0.0000089	0.00517
	regulation of cell-substrate adhesion	12.44	0.0000534	0.01870
	extracellular matrix organization	12.31	0.0000094	0.00531
	external encapsulating structure organization	12.26	0.0000096	0.00523
	extracellular structure organization	12.26	0.0000096	0.00506
	regulation of epithelial cell migration	11.55	0.0000753	0.02370
*	angiogenesis	10.15	0.0000274	0.01110
	negative regulation of locomotion	9.96	0.0000304	0.01190
	heart development	9.73	0.0000001	0.00013
	negative regulation of cell migration	9.71	0.0001670	0.03810
	negative regulation of cell motility	9.29	0.0002050	0.04420
	negative regulation of cellular component movement	9.01	0.0002350	0.04680
*	blood vessel morphogenesis	8.77	0.0000139	0.00685
	positive regulation of cell adhesion	8.73	0.0000143	0.00684
	blood circulation	8.01	0.0001000	0.02920
	regulation of anatomical structure size	7.72	0.0000079	0.00494
	regulation of cell adhesion	7.5	0.0000006	0.00064
	circulatory system process	7.45	0.0001480	0.03480

*	blood vessel development	7.11	0.0000519	0.01860
	regulation of neuron projection development	7.05	0.0000549	0.01880
*	vasculature development	6.74	0.0000726	0.02330
	circulatory system development	6.55	0.0000006	0.00063
	positive regulation of locomotion	6.39	0.0001010	0.02880
	tissue morphogenesis	6.16	0.0001270	0.03220
	negative regulation of multicellular organismal process	6.07	0.0000003	0.00045
	tissue development	5.91	0.0000000	0.00000
	cell adhesion	5.85	0.0000177	0.00821
	regulation of cell migration	5.85	0.0000055	0.00378
	biological adhesion	5.78	0.0000194	0.00851
	regulation of cell motility	5.55	0.0000087	0.00526
	regulation of response to external stimulus	5.54	0.0000271	0.01120
	regulation of locomotion	5.3	0.0000131	0.00664
*	anatomical structure formation involved in morphogenesis	5.22	0.0000427	0.01600
	regulation of cellular component movement	5.11	0.0000178	0.00801
	cell migration	4.97	0.0001700	0.03820
	regulation of apoptotic process	4.87	0.0000012	0.00103
	animal organ morphogenesis	4.81	0.0000807	0.02490
	negative regulation of apoptotic process	4.77	0.0002240	0.04530
	regulation of programmed cell death	4.75	0.0000015	0.00122
	epithelium development	4.73	0.0000914	0.02720
	negative regulation of programmed cell death	4.67	0.0002610	0.04900
	regulation of cell population proliferation	4.55	0.0000009	0.00088
	animal organ development	4.37	0.0000000	0.00000
	regulation of cell death	4.29	0.0000048	0.00360
*	anatomical structure morphogenesis	4.13	0.0000001	0.00023
	movement of cell or subcellular component	3.78	0.0002190	0.04550
	cell development	3.64	0.0000617	0.02070
	regulation of multicellular organismal process	3.55	0.0000005	0.00062
	system development	3.29	0.0000000	0.00001
	cell differentiation	3.24	0.0000001	0.00025
	cellular developmental process	3.2	0.0000002	0.00026
	multicellular organism development	2.99	0.0000000	0.00001
	anatomical structure development	2.98	0.0000000	0.00000
	developmental process	2.87	0.0000000	0.00000
	negative regulation of cellular process	2.62	0.0000012	0.00107
	negative regulation of biological process	2.4	0.0000058	0.00382
	positive regulation of cellular process	2.33	0.0000052	0.00375
	positive regulation of biological process	2.32	0.0000013	0.00108
	multicellular organismal process	2.25	0.0000001	0.00017
*	cellular component organization	2.13	0.0002540	0.04880